JOURNAL OF GEOPHYSICAL RESEARCH, VOL. 102, NO. D12, PAGES 13,423–13,432, JUNE 27, 1997

The average dissipation rate of turbulent kinetic energy in the neutral and unstable atmospheric surface layer

John D. Albertson,[1] Marc B. Parlange,[2] Gerard Kiely,[3] and William E. Eichinger[4]

Hydrologic Science, University of California, Davis

Abstract. The mean rate of dissipation of turbulent kinetic energy is related to the surface fluxes of momentum and heat through the turbulent kinetic energy budget equation. This relationship may be used to estimate surface fluxes from measurements of the dissipation rates. The success of recent applications of the approach has been limited by uncertainties surrounding the functional relationship between the dimensionless dissipation rates and the atmospheric stability parameter. A pair of field experiments was designed and carried out in the atmospheric surface layer to identify this functional relationship over a broad range of neutral and convective flows, covering greater than 3 orders of magnitude in the stability parameter. Mean dissipation rates were computed using Fourier power spectra, second-order structure functions, and third-order structure functions. Arguments are presented for the superiority of the third-order approach. A three-sublayer conceptual model is invoked to guide the dimensional analysis, and the resulting dissipation rates are shown to scale uniquely in the three sublayers. Near the wall, in the dynamic sublayer, dissipation is significantly less than production, as energy is transported up to the more convective regions, where an equality between dissipation and production is achieved.

1. Introduction

The atmospheric boundary layer (ABL) is the portion of the atmosphere which is affected directly by the land surface. Flows in the atmospheric surface layer (ASL), the lowest 10% or 100 m of the daytime convective ABL, are directly dependent on the surface fluxes of momentum and heat, which are the production sources of turbulent kinetic energy (TKE). The mean TKE dissipation rate (ε) is related to the production rate of TKE, and hence the surface fluxes, through the TKE budget equation. Using the relation between ε and the surface fluxes, measurements of ε can be used to obtain the surface fluxes of momentum and sensible heat for practical applications [e.g., *Fairall and Larsen*, 1986; *deLeonibus and Simpson*, 1987; *Skupniewicz and Davidson*, 1991; *Edson et al.*, 1991; *Eichinger et al.*, 1993; *Albertson, et al.*, 1996; *Kiely et al.*, 1996]. This flux-dissipation technique, first suggested by *Deacon* [1959], is very useful over oceans, where the proper vertical alignment of instruments for eddy correlation is all but impossible. It is also ideally suited for use with optical remote sensing instruments. However, the efficacy of this method depends on empirical formulae to describe the role of atmospheric stability (or stratification) on the relationship between ε and the surface fluxes. There exists considerable uncertainty in the literature regarding the scaling of ε in the atmospheric surface layer under neutral and unstable atmospheric stability. In this paper, new experimental results are presented on the scaling of the average dissipation rate of TKE with respect to stability; these results are analyzed in the context of a directionally referenced form of Monin-Obukhov similarity theory [e.g., *Bechtov and Yaglom*, 1971; *Zilitinkevich*, 1971; *Kader and Yaglom*, 1990] to identify improved scaling laws that will support and improve the accuracy of future applications of the flux-dissipation methods. The improved understanding of how TKE dissipation scales with stability (or dimensionless height) in the ABL is also of basic importance to dissipation-based closure models used in numerical simulation of boundary layer flows.

The TKE budget equation is obtained by multiplying the momentum equation for the x_α (α = 1 (streamwise), 2 (lateral), 3 (vertical)) direction by u_α, time averaging all terms, and subtracting the equation governing the kinetic energy of the mean flow [see *Tennekes and Lumley*, 1972, pp. 63-64]. We maintain the convention of using Greek letters for directional subscripts, U_α for the mean velocity in the α direction, and u_α for fluctuations in the α direction velocity about its mean value. Furthermore, as our interest is in the ASL, we must account for temperature stratification and the accompanying buoyant forces [*Monin and Yaglom*, 1971, p. 418]. For a steady state flow with horizontal homogeneity, we write the TKE budget per unit mass with the Boussinesq approximation as

$$-\langle u_1 u_3 \rangle \frac{\partial U_1}{\partial x_3} + \frac{g \langle u_3 t_v \rangle}{T_v} - \left(\frac{1}{2}\right) \frac{\partial \langle u_\alpha u_\alpha u_3 \rangle}{\partial x_3} - \left(\frac{1}{\rho}\right) \frac{\partial \langle p u_3 \rangle}{\partial x_3} = \varepsilon \quad (1)$$

[1]Now at Department of Environmental Sciences, University of Virginia, Charlottesville.

[2]Now at Department of Geography and Environmental Engineering, The Johns Hopkins University, Baltimore, Maryland.

[3]Permanently at Department of Civil Engineering, University College, Cork, Ireland.

[4]Now at Institute of Hydraulic Research, University of Iowa, Iowa City.

Paper number 96JD03346.
0148-0227/97/96JD-03346$09.00

where t_v and p represent fluctuations about the mean virtual temperature T_v and the mean pressure, respectively, g is the gravitational acceleration, ρ is the density of air, and summation is implied on repeated subscripts. For convenience, we are using virtual temperature to capture the combined effect of air temperature and water vapor fluctuations on the density [e.g., *Brutsaert*, 1982, p. 37]. The first term in (1) represents the mechanical production of TKE by interaction of the Reynolds stress and the mean velocity gradient, the second term represents the production of TKE by buoyant forces, the third term is the divergence of vertical turbulent flux, the fourth term is the transfer of TKE due to pressure-velocity interaction, and the last term represents the dissipation (destruction) of TKE by viscous action. It is important to note that (1) is a time-averaged equation which is not sensitive to the particular distribution of the instantaneous dissipation rate, which is known to be highly intermittent [e.g., *Kraichnan*, 1991; *Meneveau and Sreenivasan*, 1991].

The friction velocity (u_*) is defined as

$$u_* = \sqrt{\frac{\tau_o}{\rho}} = \sqrt{- < u_1 u_3 >} \tag{2}$$

where τ_o is the surface shear stress. Substituting (2) into (1), and writing F for the flux divergence term and P for the pressure velocity term gives

$$u_*^2 \frac{\partial U_1}{\partial x_3} + \frac{g < u_3 t_v >}{T_v} - F - P = \varepsilon \tag{3}$$

We use the dimensionless atmospheric stability parameter (z/L), where

$$L = \frac{- u_*^3 T_v}{kg < u_3 t_v >} \tag{4}$$

is the Obukhov length and k(=0.4) is von Karman's constant. The mean velocity gradient from Monin-Obukhov similarity is given as

$$\frac{\partial U_1}{\partial x_3} = \frac{u_*}{kz} \phi_m \left(\frac{z}{L} \right) \tag{5}$$

where ϕ_m is the nondimensional velocity gradient which depends on (z/L). Substitution of (5) into (3) and multiplying by kz/u_*^3 yields the nondimensional TKE budget.

$$\phi_m \left(\frac{z}{L} \right) - \frac{z}{L} - \frac{Fkz}{u_*^3} - \frac{Pkz}{u_*^3} = \phi_\varepsilon \left(\frac{z}{L} \right) \tag{6}$$

where $\phi_\varepsilon(z/L)$ represents the nondimensional dissipation rate as a function of stability. The function $\phi_m(z/L)$ is relatively well established for most values of (z/L) typically found in the field [*Businger, et al.*, 1971; *Dyer*, 1974; *Brutsaert*, 1992; *Parlange and Brutsaert*, 1993; *Parlange and Katul*, 1995]. The form, or behavior, of ϕ_ε, F, and P relative to z/L is considerably less clear.

The ϕ_ε should be a universal function of the stability parameter (z/L), as defined by Monin-Obukhov similarity theory. An important point to note here is that the mean dissipation rate of TKE should not be susceptible to the same contamination from large convective eddies as is the longitudinal velocity variance [e.g., *Garratt*, 1992, p. 72]. The large-scale, boundary layer filling convective eddies that cause σ^2_u to deviate from the Monin-Obukhov predictions are constrained to the low-wavenumber end of the power spectrum. These eddies significantly affect the variance, i.e., area under the power spectrum. However, as these eddies are limited to the low-wavenumber range, the inertial subrange should not be affected by their presence or absence. Recall that the mean dissipation rates are tied to the intercept of the straight-line fit through the inertial subrange scaling [*Kolmogorov*, 1941] and will therefore not be affected.

To estimate the momentum flux from (6) using measurements (either direct or inferred) of ε, the dependency of ϕ_ε on z/L must be known with considerable level of confidence. Generally, for flux calculations, F and P have been assumed to be negligible with respect to the production and dissipation terms, thus implying an equality between production and dissipation. As *Tennekes and Lumley* [1972, pp. 64-65] point out, we should expect an equality of dissipation and production when integrating over the depth of the boundary layer, but not necessarily at any one point in a shear flow. As production and dissipation are nearly always of the same order of magnitude, it may be conceptually appealing to assume an equality; however, this may not be appropriate for quantitative applications. The transport terms have been assumed to balance the budget equation when measurements of dissipation exceeded production [e.g., *Wyngaard and Coté*, 1971; *Hogstrom*, 1990] or when production exceeded dissipation [e.g., *Frenzen and Vogel*, 1992]. The relative value of production versus dissipation for different stability (z/L) values is uncertain. We review briefly the literature on the relationship between production and dissipation, with attention given to the stability ranges encountered during various field experiments.

Wyngaard and Coté [1971] measured mechanical and buoyant production, dissipation, and the flux divergence during the Kansas Experiment. They found a flux divergence of TKE for every unstable stability case. They claimed that the vertical turbulent transport of TKE completely offsets the amount produced by buoyant action. Their results show dissipation exceeding production for moderately unstable flows, with an equality approached for more strongly convective flows. However, inclusion of the measured flux divergence term caused a considerable imbalance in the TKE budget. They extrapolated their fit to assume an equality between dissipation and production in the neutral limit. Their data do not include low enough $-z/L$ values to confirm this assumption, as only three runs with $-z/L<0.1$ were analyzed. They fit an empirical function to their data,

$$\phi_\varepsilon \left(\frac{z}{L} \right) = \frac{\varepsilon kz}{u_*^3} = \left(1 + 0.5 \left| \frac{z}{L} \right|^{\frac{2}{3}} \right)^{\frac{3}{2}} \tag{7}$$

which approaches unity in the neutral limit and scales linearly with $|z/L|$ in the free convective limit ($-z/L \gg 1$). For the unmeasured P term in (6), Wyngaard and Coté extended and earlier analysis by *Batchelor* [1951] and estimated the magnitude of Pkz/u_*^3 to be about 0.9 for $z/L = -1.0$, which is of the order of the imbalance they reported. Wyngaard and Coté suggested in conclusion that the pressure-velocity covariance term may be important, but that direct measurements of it are necessary before its true role will become clear. With present instrumentation, it is exceedingly difficult to measure the gradients of pressure-velocity interaction in the ABL. The numerical simulation of ABL flows is showing promise, and with advancements in computational capabilities, we may soon be able to study the near-wall region with high-resolution meshes and learn more about these hard to measure terms.

In a study of the TKE budget in the ASL over grass, *McBean et al.* [1971] found dissipation to match production in the near-neutral cases, and to exceed production for unstable atmospheric stability when $-z/L > 0.3$, up to a maximum difference of about 70% for the highly unstable cases. They attribute these results to an increasing importance of the turbulent energy flux term (F) in the ASL below $z = 2$ m for more unstable stability conditions (i.e., higher $-z/L$ values), though F was not measured in their study. *McBean and Elliot* [1975] studied the F and P terms over a dry prairie and found them to have significant and counteracting effects on the TKE budget, with F removing and P adding energy at the measurement height. The net effect was a near equality of local production and dissipation for the stability range measured. Their data were collected with a maximum $-z/L$ of 0.5, and there were only four measurements taken with $-z/L$ below 0.05. Interestingly, they concluded that Monin-Obukhov similarity theory may not hold for the vertical flux of TKE.

Leavitt and Paulson [1975] studied the TKE budget over the ocean during the Barbados Oceanographic and Meteorological Experiment (BOMEX) and concluded that dissipation equaled production, although their experimental scatter was about ± 50% of production. Their analysis is of data covering atmospheric stabilities ranging from z/L of -0.14 to -1.5. They also estimated the vertical turbulent flux divergence (the nondimensionalized F) and found it to be greater than zero and to increase with increasing $-z/L$. This term was found to be about one half as large as the buoyant production, in contrast to *Wyngaard and Coté's* [1971] result that the F term was equal to buoyant production.

Champagne et al. [1977] studied the TKE budget and used the measured dissipation rates to estimate surface fluxes from a furrowed bare soil surface in Minnesota for a narrow atmospheric stability (z/L) range of -0.067 to -0.11. They used the assumptions of *Wyngaard and Coté* [1971] and found dissipation to generally exceed production. As with the Kansas Experiment, *Champagne et al.* [1977] attribute an imbalanced TKE budget to the uncertainty of the pressure transport term.

Hogstrom [1990] inferred dissipation rates from inertial subrange analysis of Fourier power spectra for measured longitudinal velocity time series and identified the vertical flux divergence of TKE with measurements at multiple heights. His inertial subrange estimates showed the near-neutral TKE dissipation to be about 25% larger than the rate of production, and his flux divergence measurements showed the F term to be removing about 25% of production upward from the measurement height. He did not measure the pressure term (P), but estimated that it must be contributing 50% of production to close the TKE budget, which he explained as being due to "inactive" eddy motion. We should note that changing the value of the Kolmogorov constant used in *Hogstrom's* [1990] analysis from 0.52 to the 0.55 value used in this study would reduce his dissipation rates to just 14% greater than production. *Hogstrom* [1990] also modified the results of *Wyngaard and Coté* [1971] to correct for flow distortion, which revealed that the Kansas Experiment results have dissipation less than TKE in the near-neutral regime.

In another study, *Frenzen and Vogel* [1992] performed an experiment over emerging wheat in Wyoming and found dissipation to be 15 to 20% less than production. They also mention that by removing some "corrections" made to the Kansas data by *Wyngaard and Coté* [1971], near-neutral dissipation is found to be less than production.

This brief review is indicative of the persistent uncertainty associated with the scaling of ϕ_ε with atmospheric stability (z/L). Most of this uncertainty is ignored in flux-dissipation applications, and the dissipation of TKE is simply assumed to equal the production. This is a potentially perilous assumption in light of *Tennekes and Lumley's* [1972] remarks concerning the likely inequality of production and dissipation at any arbitrary point in a shear flow. Furthermore, some of the uncertainty must be attributed to data processing techniques and the variability in values assumed for Kolmogorov's inertial subrange constant. We could approach this problem by attempting to measure the production, turbulent transport, and pressure transport terms to define the dissipation rate as the residual (including the additive measurement errors of the other terms). Instead, we take a more direct approach of studying just the dimensionless dissipation rate in order to refine its scaling with respect to stability as needed to improve the accuracy of flux-dissipation applications. The resulting scaling function will also be useful as a basic understanding necessary for dissipation-based closure schemes in numerical simulations of boundary layer flows. The present effort considers fast response atmospheric surface layer velocity measurements, collected over a broad range of atmospheric stability, in the framework of directional dimensional analysis (DDA).

2. The Three-Sublayer Model and Directional Dimensional Analysis

Bechtov and Yaglom [1971], building on the work of *Zilitinkevich* [1971] and the DDA first applied to the ASL by *Bernstein* [1966], presented a three-sublayer model of the unstably stratified boundary layer. *Kader and Yaglom* [1990] published a broad experimental examination of this theory using data collected in the ASL over a 7-year period. More recently, *Zilitinkevich* [1994] extended the theory to accommodate the top-down/bottom-up scaling concept of *Wyngaard* [1983].

As opposed to classical dimensional analysis, DDA involves different length scales for the different directions, such as L_x for horizontal and L_z for vertical lengths [see *Panton*, 1984, pp. 207-209; *Kader and Yaglom*, 1990]. The addition of basic dimensions will decrease the number of dimensionless groups that can be formed from the basic physical parameters, in accordance with Buckingham's pi theorem. This may sharpen the result, as it yields explicit functional forms for the terms in the TKE budget with known exponents, rather than the classical similarity theory with the empirical scaling components. To apply this approach, the processes in the different directions must be essentially independent of each other [*Panton*, 1984], or as *Kader and Yaglom* [1990] put it, the horizontal and vertical motions must be uncoupled. Here enters the need for the three-sublayer model.

The basic concept of the ASL being represented by three distinct sublayers [*Bechtov and Yaglom*, 1971] did not receive substantial experimental support until recently [e.g., *Kader*, 1988; *Kader and Perepelkin*, 1989; *Kader and Yaglom*, 1990]. The lowest of the three sublayers is termed the dynamic sublayer (DSL) and is defined to be that region where the buoyant production is negligible with respect to mechanical production of TKE. Just above this sublayer is the so-called dynamic-convective sublayer (DCSL), where buoyant production becomes relevant and must be considered along with the still important mechanical production. The uppermost portion of the ASL, just

above the dynamic-convective sublayer, is the free convection sublayer (FCSL), which is affected strictly by the buoyant forces. The DDA is useful, as the buoyant forces act in the vertical direction and the shearing action is in the horizontal direction, giving these two energy terms different dimensions. The DSL represents the neutral limit ($z << -L$), and the FCSL the free-convective limit ($z >> -L$). However, the DCSL does not fit as cleanly into the classical similarity theory approach. In this middle region, the theory states that the transfer of energy between the horizontal and vertical velocity fluctuations is small with respect to the rates of mechanical production of energy in the horizontal direction and buoyant production in the vertical direction [*Kader and Yaglom*, 1990]. The energy transfer between the horizontal and vertical motions is neglected, and the vertical and horizontal motions are considered to be energetically uncoupled, thus allowing for the applications of DDA. The predicted scaling of the individual terms in (6) for each of the three sublayers is discussed next, with the expected stability ranges of the sublayers based on the order of magnitude analysis of *Kader* [1992].

2.1. Dynamic Sublayer ($-z/L < 0.04$)

All one-point moments are believed to be independent of z in the dynamic sublayer [*Kader and Yaglom*, 1990; *Kader*, 1992], so the derivatives F and P are expected to vanish. The buoyant production is negligible compared to mechanical production in this sublayer, and the normalized mechanical production ϕ_m assumes a value of unity. This leaves the normalized dissipation rate ϕ_ε, which, according to dimensional analysis, should be constant in the dynamic sublayer, i.e., independent of z. If F and P are in fact equal to zero, and ϕ_m is equal to unity, then ϕ_ε should also be equal to unity in this lowest sublayer. So we would expect

$$\phi_\varepsilon = C_1 \approx \phi_m = 1 \tag{8}$$

where C_1 is a constant. However, as discussed above, most experimental evidence suggests a departure of ϕ_ε from 1, while still supporting that $\phi_m = 1$. This inequality between ϕ_ε and ϕ_m implies that the one-point moments of F and P may not vanish in this sublayer. *Hogstrom* [1990] showed F to be a nonzero constant in this flow regime, thus allowing ϕ_ε to be not equal to ϕ_m, while still maintaining that ϕ_ε is a constant. In consideration of uncertainty here, *Kader* [1992] called for additional experimental work in this sublayer to improve the ϕ_ε (z/L) formulation.

2.2. Dynamic-Convective Sublayer ($0.12 < -z/L < 1.2$)

In the dynamic-convective layer the DDA is useful, since there is distinct action in both the horizontal and vertical directions, such that the analysis becomes more complex than in the other layers (where conventional dimensional analysis will yield the same results as DDA). In addition, the F and P terms can be important in this middle layer. Following DDA, the friction velocity u_* has dimensions $[Lx^{1/2}\ Lz^{1/2}\ t^{-1}]$, which is not completely appropriate for scaling the horizontal (x direction) motions. Therefore the local convective velocity $w_*(=[\langle u_3 t_v \rangle g z/T_v]^{1/3})$ with dimensions $[L_z t^{-1}]$ is used to scale the vertical motion, and the combination u_*^3/w_* with dimensions $[L_x t^{-1}]$ is used to scale the horizontal motion. Applying these scaling velocities to the appropriate terms in (1), following pure dimensional arguments, yields

$$\phi_\varepsilon = C_2\left(\frac{-z}{L}\right)^{\frac{-1}{3}} + \left(1 - C_3\right)\left(\frac{-z}{L}\right) \tag{9}$$

where C_2 is a constant that describes both the positive effect of mechanical production and the vertical transport of u_1u_1 and u_2u_2 energy (negative); the value of 1 that accompanies C_3 accounts for buoyant production; and the constant C_3 captures the vertical transport of the u_3u_3 energy as well as the effect of pressure-velocity interaction. For a more detailed derivation of (9) from (1), see *Kader* [1992]. *Zilitinkevich* [1994] provides additional discussion about this intermediate regime.

2.3. Free Convection Sublayer ($-z/L > 2$)

For free convection scaling the flow variables should be independent of u_* and should instead depend on the convective velocity scale w_*. Hence ϕ_m scales with $(-z/L)^{1/3}$, and the remainder of terms on the left-hand side of the TKE budget scale with $(-z/L)^1$. From dimensional analysis

$$\phi_\varepsilon = C_4\left(\frac{-z}{L}\right)^{\frac{1}{3}} + C_5\left(\frac{-z}{L}\right) \tag{10}$$

where the constant C_4 describes the contribution of mechanical production and C_5 reflects a sum of constants which individually represent buoyant production, F, and P. Note that C_4 can be neglected in this sublayer, as mechanical production is becoming small with respect to buoyant production. Again, we refer to *Kader* [1992], where the derivation of these scaling forms is already published.

3. Determination of ε

For a velocity signal, ε may be computed by either so-called "direct" or "indirect" methods. The direct methods are typically based on an assumption of local isotropy, to eliminate the need to measure all the terms in the dissipation rate tensor and relate simply ε to the squared longitudinal velocity derivative, viz.,

$$\varepsilon = 15\upsilon\left\langle\left(\frac{\partial u_1}{\partial x_1}\right)^2\right\rangle \tag{11}$$

In practice, (11) may be implemented by differentiating the temporal velocity signal and invoking Taylor's [1938] hypothesis of frozen turbulence, or by evaluating the curvature of the autocorrelation function about the origin at zero lag to provide an estimate of the Taylor microscale λ, which yields the dissipation rate [see *Tennekes and Lumley*, 1972, pp. 210-211]

$$\varepsilon = 15\upsilon\frac{\left\langle u_1^2\right\rangle}{\lambda^2} \tag{12}$$

The indirect methods are based on *Kolomogorov*'s [1941] (hereafter K41) second hypothesis, which relates the velocity difference (Δu_α) between two points separated by a distance r directly to ε and r, where it is required that r be much smaller than the production scales and much larger than the viscous scales (i.e., r must be in the inertial subrange). This cornerstone of turbulence analysis provides, in theory, myriad ways of computing ε from time series of longitudinal velocity. In the present study, we focus on three of these: (1) power spectra, (2) second-order structure functions, and (3) third-order structure

functions. For simplicity, we write $\Delta u_i(r)$ for the velocity difference between two points separated by a distance r, and by necessity, we use Taylor's [1938] hypothesis of frozen turbulence for expressing temporal velocity data taken at a single point as spatial data [e.g. *Tennekes and Lumley*, 1972, p. 253]. The second-order structure function represents the average squared velocity differences $D_2(r)\equiv\langle(\Delta u_i(r))^2\rangle$, and the third-order structure function uses cubed velocity differences $D_3\equiv(r)\langle(\Delta u_i(r))^3\rangle$ [see *Monin and Yaglom*, 1975, chap. 8]. Following K41, dimensional analysis yields directly the following expressions for the second- and third-order structure functions in the inertial subrange:

$$D_2(r) = S_2\varepsilon^{\frac{2}{3}}r^{\frac{2}{3}} \qquad D_3(r) = -\frac{4}{5}\varepsilon r \tag{13}$$

where S_2 is an empirical constant and the -4/5 constant of the third-order structure functions is an exact result from the equations of motion and the work of *von Karman and Howarth* [1938]. (Subsequent to the original submission of this manuscript, *Frisch* [1995] referred to this exact result as "... one of the most important results in fully developed turbulence as it is both exact and nontrivial.") The Fourier counterpart of the second-order structure function is the power spectrum, which is described in the inertial subrange following K41 as

$$E_{u_i}(k_x) = \alpha_u\varepsilon^{\frac{2}{3}}k_x^{\frac{-5}{3}} \tag{14}$$

where $E_{ui}(k_x)$ describes the expected energy content of turbulent velocity fluctuations at wavenumber k_x (rad/m) and α_u is an empirical constant. Note that k_x and r are related as $k_x = 2\pi/r$, and the empirical constants α_u and S_2 are related under a constant skewness assumption as $S_2 = 4.02\alpha_u$ [e.g., *Anselmet et al.*, 1984]. An important distinction between the second- and third-order moments is that the former are subject to intermittency corrections and include empirically determined constants, while the latter has an exact constant and is immune to intermittency effects in its inertial subrange scaling [e.g., *Anselmet et al.*, 1984; *Frisch*, 1995]. There remains some concern about application of the second-order approaches to define dissipation rates from inertial subrange measurements, as the average of the two-thirds power of the instantaneous dissipation rate can be quite different from the two-thirds power of the average dissipation rate. The third-order approach is linear in ε and will therefore not suffer from these concerns or ambiguities.

4. Experiment

Surface energy balance and atmospheric turbulence measurements were conducted at two sites: a bare soil field located at the Campbell Tract research facility on the campus of the University of California, Davis and the dry Owens Lake bed, in Owens Valley, California. A one-dimensional sonic anemometer with a fine-wire (diameter 0.0127 mm) thermocouple and a Krypton hygrometer were used (at 10 Hz with covariances taken over 20-min periods) to measure the vertical fluxes of sensible and latent heat. A three-dimensional sonic anemometer (Gill Instruments 1012R2) with transponder spacing of 15 cm was used to measure and record the three velocity components, at 21 Hz for the Campbell Tract site and 56 Hz for the Owens Lake site. The eddy correlation equipment ran continuously for each day of the experiment on the 20-min averaging time step. The three-dimensional sonic was run for up to 12 hours continuously each day, with signals written to a new file each 20 min (i.e., 25,200 points at 21 Hz and 67,200 points at 56 Hz) for ease in data processing and time matching to the energy balance measurements.

4.1. Campbell Tract

Campbell Tract is a plowed field extending 500 by 500 m, with an irrigation system capable of saturating a portion of the field extending 155 m in the north-south direction and 115 m in the east-west direction. The irrigated plot is located in the northeast corner of the main field. The surface roughness length has been estimated to be $z_0 = 2$ mm, and the prevailing winds are out of the southwest. Data were collected at $z = 0.85$ m on June 22, 23, and 24, 1994, and at $z = 1.5$ m on July 15, 16, and 17, 1994. Irrigations were performed over the nights of June 21 and July 14, 1994, with periods of drying in between. Saturating the soil surface extends the range of the DSL available for experimental investigation, since most of the available energy is partitioned to latent heat rather than sensible heat. This provides for a wide range of atmospheric stability conditions. The days immediately following an irrigation provide typically low values of $-z/L$ as most of the available energy at the surface is used for evaporation. The value of $-z/L$ increases with time following an irrigation, as more energy is partitioned to sensible heat flux, thereby increasing the buoyant production of TKE.

4.2. Owens Lake

The dry Owens Lake bed is located in the southern portion of the Owens Valley. Its surface area exceeds 200 km^2. It is bounded on the west by the Sierra Nevada and on the east by the Inyo Mountains. The surface consists of crusted sand and evaporative salts, with a roughness length estimated at $z_0 = 0.13$ mm [*Katul, et al.*, 1995] and uniform fetch exceeding 10 km. The predominant wind during the experiment was out of the southwest. Samples were taken of the surface crust soil, exposed to a chilled mirror hygrometer test in the Desert Research Institute's laboratory, and found to have gravimetric moisture contents below 1% (W. Albright, personal communication, 1995). These site conditions provide for strongly convective flows that present a wide range of stability in the FCSL for examination. Data were collected over Owens Lake from August 8 through 12, 1994, at a measurement height of $z = 2.65$ m.

The data files were screened for suitability of Taylor's hypothesis-based conversion from the temporal to spatial domain on the basis of turbulence intensity ($TI = \sigma_{ui}/U_i$). Our analysis revealed the scaling of the dimensionless dissipation rate to be insensitive to TI for values of TI < 50%. Therefore a TI < 50% cutoff was imposed for an unambiguous decomposition of each signal into a mean and fluctuating component for the computation of dissipation rates [see *Stull*, 1988, p. 6; *Kiely* et al., 1996]. The TI cutoff reduced the 183 files collected at the Campbell Tract to 113, and the 103 files collected at Owens Valley to 75, yielding a total of 188 files for analysis, each representing a 20-min measurement period.

After rotating the coordinate system into the mean wind for each file and subtracting the mean values, the friction velocity u_* was calculated from the resultant surface stress as [*Stull*, 1988, p. 67]

$$u_* = \left(\left\langle u_1u_3\right\rangle^2 + \left\langle u_2u_3\right\rangle^2\right)^{\frac{1}{4}} \tag{15}$$

The use of (15) did not give appreciably different results from those from the longitudinal stress ($u_* = -\langle u_1u_3\rangle^{1/2}$). The stability

parameter was computed using (4) with heat fluxes from the eddy correlation instruments and friction velocity from the three-dimensional sonic anemometer. Note that the signals were not detrended, as the TI cutoff effectively captured and discarded files with nonstationary means. The atmospheric stability encountered during the acceptable TI portion of the experiment ranged over more than 3 orders of magnitude: $0.004 < -z/L < 8.1$.

The power spectrum of the longitudinal velocity component of each file was computed to support the estimation of ε from (14). This involved the square windowing of 2048 points from the file, Bell tapering [*Stull*, 1988, pp. 308-310] the first and last 10% of the window, computing the power spectrum of the window, repeating this process on the remaining windows (2048 each) in the file, and averaging the energy of all windows for each wavenumber. This process resulted in averaging of the power spectra for at least 10 windows in each file.

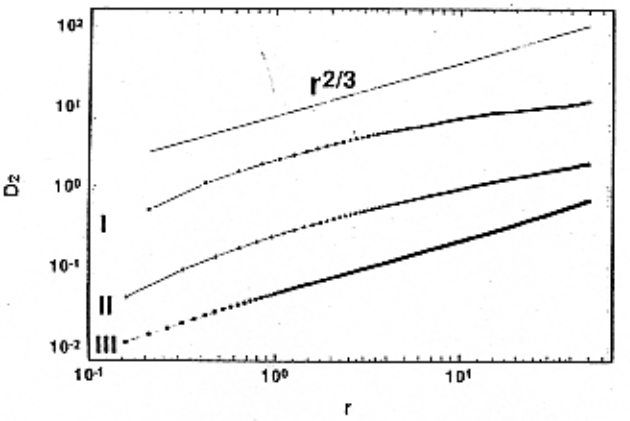

Figure 1b. Second-order structure functions for the same three sample files shown in Figure 1a. D_2 has units of m^2/s^2 and r has units of m.

5. Results and Discussion

Space limitations preclude the graphical presentation of the spectra and structure functions for all 188 files. However, it is instructive to examine the appearance of these plots, so figures are included for three files, representing a DSL flow (I: $z/L = -0.03$), a DCSL flow (II: $z/L = -0.39$), and a FCSL flow (III: $z/L = -4.0$). These files have their power spectra presented in Figure 1a, second-order structure functions in Figure 1b, and third-order structure functions in Figure 1c. Note that the spectra follow the -5/3 inertial range scaling for a reasonably wide range of k_x, in fact, for a range considerably wider that that which could strictly be defined as an inertial subrange. As our objective of the inertial range analysis is to identify the dissipation rate from the intercept, we can rest on this rather weak but necessary condition for inertial subrange scaling. We expect the strict inertial subrange for the longitudinal velocity to correspond to scales that are smaller than one-half the measurement height (large structure end) and larger than the scale at which path-averaging effects of the sonic anemometer become critical (small structure end) [see *Kaimal et al.*, 1968; *Kaimal*, 1986; *Wyngaard*, 1986]. However, since long-standing empirical evidence shows the longitudinal power spectra to possess a linear -5/3 scaling (in the log-log framework) over a wider range than the narrow, strictly defined inertial subrange, we can readily regress a range of the measured scales with the prescribed slope of -5/3 to identify the intercept as needed to estimate ε. These calculations are based on observations in a narrow range of scales that fall between the measurement height and the scale at which path averaging effects become important. We must note that for studies of flow properties other than the local structure of the longitudinal velocity component, a higher instrument placement may be necessary to ensure the presence of a strict inertial subrange. We refer to *Kaimal et al.* [1986] for guidance on this issue.

Log transformation of (14) allows for determination of ε from the regressed intercept of $\log(E)$ versus $\log(k_x)$ over a range of wavenumbers in the inertial subrange, using α_{u1}=0.55. While there is no strong consensus on the exact value of α_{u1}, 0.55 falls near the median of the published estimates [*Deacon*, 1988; *Kaimal and Finnigan*, 1994]. These estimates of ε derived from the power spectra of the 188 runs and normalized to u_*^3/kz (i.e., ϕ_ε) are shown in relation to the stability parameter (z/L) in Figure 2a. Vertical bars are included in the figure to delineate the DSL, DCSL, and FCSL. Similarly, log transformation of (13), and the selection of $S_2 = 2.2$ ($= 4.02*\alpha_{u1}$) in accordance with the

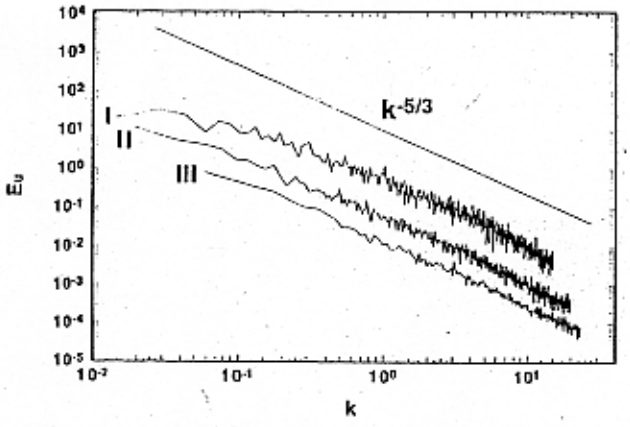

Figure 1a. Power spectra of streamwise velocity fluctuations (u_1') for three sample data files. I represents DSL, II DCSL, and III FCSL. The spectrum has units of m^3/s^2, and the wavenumber k (k_X in the text) has units of m^{-1}. The spectra have been shifted apart for presentation, so the absolute magnitudes of E_u should be disregarded.

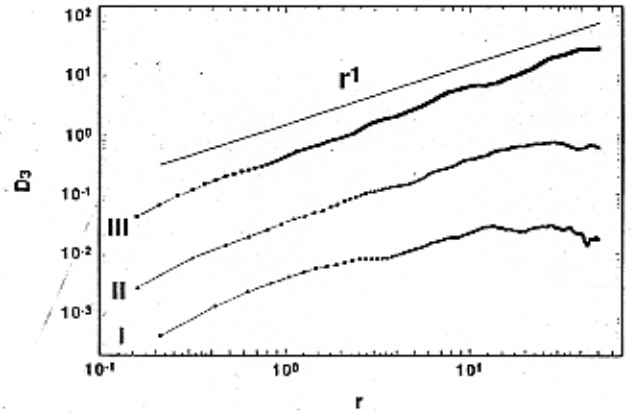

Figure 1c. Third-order structure functions for the same three sample files shown in Figure 1a. D_3 has units of m^3/s^3 and r has units of m.

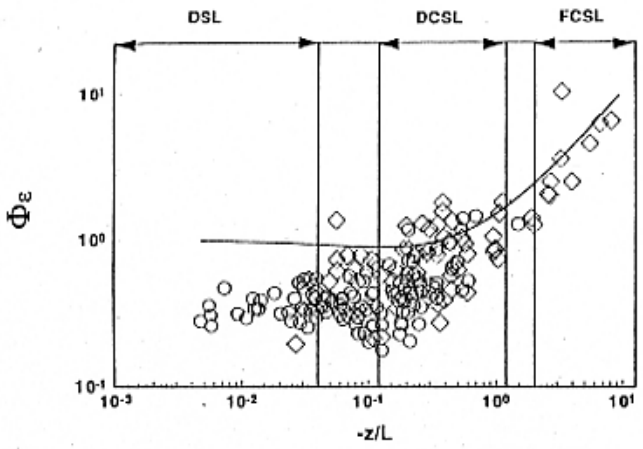

Figure 2a. Power spectra based estimates of the normalized dissipation rates versus atmospheric stability for the 188 files. The Campbell Tract points are marked by circles, and the Owens Lake points with diamonds. The estimated normalized rate of production of TKE is shown with a solid line.

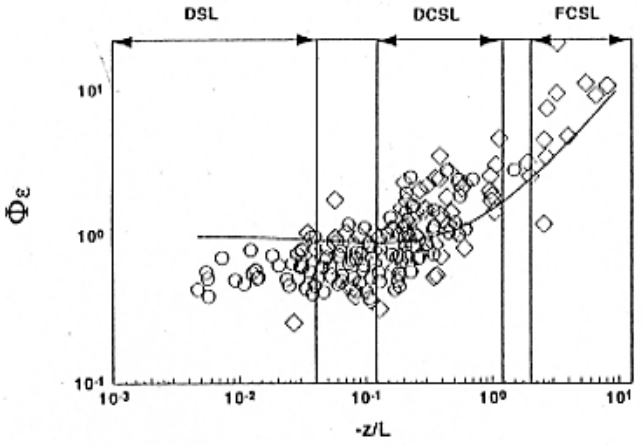

Figure 2c. Third-order structure function based estimates of the normalized dissipation rates versus atmospheric stability for the 188 files. Symbols are as in Figure 2a.

constant skewness assumption, yielded estimates of ε, which are shown in normalized form (ϕ_ε) in figures 2b and 2c for the second- and third-order structure functions, respectively. For reference, a typical estimate of the normalized production [$(1-15z/L)^{-1/4}$-z/L] is plotted along with the data on Figures 2a, 2b, and 2c [*Brutsaert*, 1982, p.68]. For consistency, we regressed the log transformed structure functions over the same range of scales as for the power spectra, although such a regression is unnecessary for the structure functions. The structure functions scale smoothly with r (cf. Figures 1b and 1c), such that a reliable estimate of ε may be computed from evaluating the structure function (13) at a single lag. In fact, this is a measure easily made by a simple field data logger, in contrast to the relatively extensive data manipulation required for the power spectra-based calculation of ε. Note that although the three methods yield estimates that differ (most likely due to the uncertain inertial subrange constants, intermittency contamination of the second-order estimates, and data treatment necessary for the power spectral scaling), they all give similar trends with respect to stability. The DSL is marked, as predicted, by an invariance of normalized dissipation with respect to z, and the break from the constant value occurs near the onset of the DCSL ($-z/L = 0.12$) as predicted by dimensional arguments [*Kader*, 1992]. The constant value is markedly below 1.0, suggesting a significant local imbalance between production and dissipation. Moreover, the imbalance is constant over the range of z/L measured in the DSL, suggesting that the transport moments are logarithmic functions of z as necessary to result in a constant divergence. This is corroborated partly by *Hogstrom's* [1990] measurements. We note that this is in contrast to the classical surface layer scaling theory, which holds that these moments are independent of z. The present finding of production exceeding dissipation throughout the large neutral region which includes more than a decade of z/L is in general agreement with the recent work of *Frenzen and Vogel* [1992] and certain reinterpretations of the Kansas experiment data of *Wyngaard and Coté* [1971]. In the DCSL and FCSL the dissipation values track more closely the estimate of production.

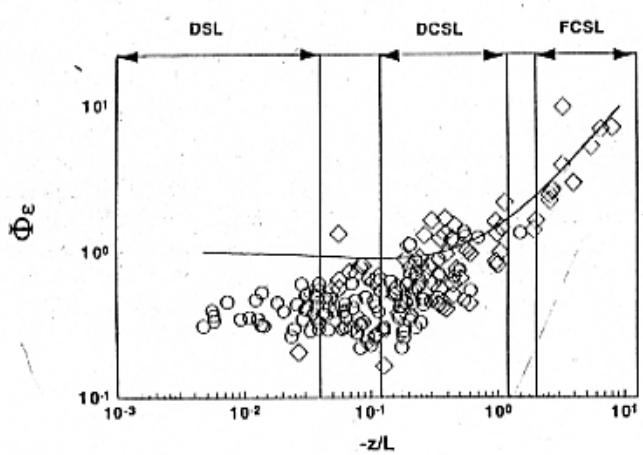

Figure 2b. Second-order structure function based estimates of the normalized dissipation rates versus atmospheric stability for the 188 files. Symbols are as in Figure 2a.

In consideration of the uncertain true values of α_u and S_2 and the susceptibility of the second-order structure function and power spectrum to intermittency effects in the inertial subrange [e.g., *Anselmet et al.*, 1984, p.77], we place more confidence in the values derived from the third-order structure function, with its exact constant (-4/5) and linear dependence on ε and associated immunity to intermittency effects. The value chosen for the Kolmogorov constant could have been modified from 0.55 to, say, 0.45 in order to bring the estimates from the second-order approaches in line with those from the third-order approach. However, little is to be gained from tuning constants when an exact inertial subrange scaling form is available (i.e., the third-order structure function scaling of Kolomogorov). To continue the analysis and narrow the scope to those estimates derived from the third-order structure functions, we introduce Figure 3, which shows the normalized mean dissipation rate over the full range of $-z/L$ computed using the third-order structure function. The original 188 data points are binned in equal log increments of $-z/L$ resulting in 14 points. The constant C_1 in (8) was computed for the third-order structure function, $C_1 = 0.61$. The DDA derived functions of (9) and (10) were fit to the unbinned third-order structure based estimates of ϕ_ε, resulting in $C_2 = 0.35$ and $C_3 = -1.28$ for the DCSL, and $C_3 = 1.81$ in the FCSL. The effect of mechanical production in the FCSL was neglected by ignoring C_4 and simply scaling ϕ_ε with $(-z/L)^1$ in this sublayer. The three-sublayer model for ϕ_ε ((8), (9), and

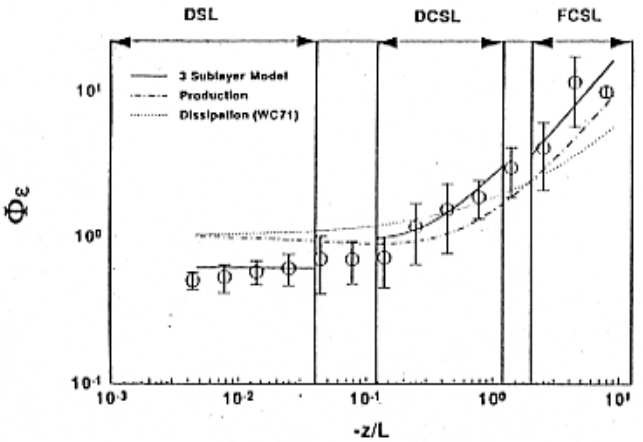

Figure 3. Data from Figure 2c placed in logarithmically spaced bins. Average of data in each bin shown with circles, and standard deviations marked with vertical bars. The three-sublayer model of (16) is shown with a solid line, estimated normalized production is shown with a dot-dash line, and *Wyngaard and Cotè's* [1971] model of dissipation is shown with a dotted line.

(10)) with constants derived from this experiment using the third-order structure function is shown as a solid line in Figure 3, representing

$$\phi_\varepsilon = 0.61 \qquad \frac{-z}{L} < 0.04$$

$$\phi_\varepsilon = 0.35\left(\frac{-z}{L}\right)^{\frac{-1}{3}} + 2.28\left(\frac{-z}{L}\right) \qquad 0.12 < \frac{-z}{L} < 1.2 \qquad (16)$$

$$\phi_\varepsilon = 1.81\left(\frac{-z}{L}\right) \qquad \frac{-z}{L} > 2$$

Also plotted is the empirical function (7) from *Wyyngaard and Cotè* [1971] marked as WC71, and a typical form of the total normalized production $[(1 - 15\ z/L)^{-1/4} - z/L]$ [e.g., *Brutsaert*, 1982, p. 68]. From Figure 3 we note (1) in the DSL the dissipation rate is significantly lower than production; (2) in the DCSL the dissipation rate closely follows but slightly exceeds production, although the difference is well within the standard deviation of the scatter; and (3) in the FCSL the dissipation rate exceeds the estimated production rate by a small amount, with the center bin point in Figure 3 pulled up by the outlier shown on the top of Figure 2c. The dissipation rate scales as predicted by the three-sublayer model based on directional dimensional analysis as identified by (16). These data may also be represented by a continuous scaling function with proper asymptotic behavior as determined by regression of the unbinned data.

$$\phi_\varepsilon = 0.61\left(1 - 2.78\frac{z}{L}\right) \qquad (17)$$

6. Conclusions

We have presented measurements representing 188 fast response velocity data files in the ASL over a wide range of atmospheric stability, spanning greater than three decades of $-z/L$. The power spectrum, second-order structure function, and third-order structure function forms of *Kolmogorov's* [1941] inertial subrange scaling were used to estimate the normalized average dissipation rate ϕ_ε of TKE. These three approaches yielded qualitatively similar results with respect to z/L, although the magnitudes differed. The power spectrum and second-order structure function approaches give similar results, while the third-order structure function approach yielded slightly higher values. The closely matched results of the two second-order methods suggests that the data treatment required for the power spectra calculations (i.e., windowing, bell tapering, and averaging) did not affect appreciably the dissipation estimates. However, the true magnitude of the second-order-based estimates may be questioned on grounds of the values chosen for α_u and S_2 and potential intermittency contamination of the inertial subrange scaling. As the third-order structure function is not prone to these problems, it is chosen as the better measure to relate ϕ_ε to z/L (see *Frisch*, [1995] for a discussion of the benefits of the third-order structure function).

The data presented represent greater than a decade of z/L in the DSL, the full DCSL, and nearly a decade of the FCSL. The predicted constant nature of ϕ_ε in the DSL was confirmed by the results. However, the magnitude of the constant (≈0.6) is substantially below unity, implying a constant local imbalance between production and dissipation of TKE. This imbalance, as in previous studies, must be attributed to the flux divergence and pressure-velocity interaction transport terms, which were not directly measured in the present study. These results suggest that the transport moments are logarithmic functions of z as measured by *Hogstrom* [1990], in contrast to the classical surface layer scaling assumption that they are independent of height. The point along the z/L axis at which ϕ_ε departs from its constant value matches closely the starting point of the DCSL, as predicted by order of magnitude analysis of the budget equation (1) [see *Kader*, 1992]. One important feature of this model is its quick transition from a constant value for ϕ_ε in the DSL to a form that grows proportional to $(-z/L)$. This quick transition is absent in the empirical model of *Wyngaard and Cotè* [1971] as well as others. However, this feature is clearly observed in our data as well as in those of *Kader* [1992]. One area in particular need of further study/validation is the left (dynamic) end of the DCSL scaling, where the model seems to miss the data. This discrepancy is visible in the work of *Kader* [1992] as well. It is emphasized that the scaling (i.e., slope) of (16) is derived completely from dimensional and physical arguments, which do not involve empirical slope fitting (as is used in (7)).

In many previous studies the actual range of $-z/L$ encountered was limited to a narrow band in the transition zone ($-z/L \approx 0.1$), yet conclusions were often inferred for the full neutral region. Figure 3 shows that the values of dissipation are close to production and similar to *Wyngaard and Cotè's* [1971] values in this narrow band. The results in Figure 3 complement and validate the partitioning of the ASL into dynamic, dynamic-convective, and free-convective sublayers. The use of a single empirical function to represent ϕ_ε throughout the ASL may fit the data, as in (17). However, the sublayer-based models provide more direct ties to the physics of the flow and are therefore better suited to dimensional arguments within the boundaries of the respective sublayers.

The three-sublayer model applied to scalar fluctuations has proven successful in the prediction of surface fluxes of sensible heat and water vapor from variances and dissipation rates measured in the surface layer [e.g. *Albertson et al.*, 1995, 1996; *Kiely et al.*, 1996]. In fact, the three-sublayer model has yielded a closed-form solution for fluxes from dissipation rates [*Albertson et al.*, 1996], thus circumventing the iterative techniques used in the past.

Considering $-z/L$ as the normalized vertical length scale, we see that close to the lower boundary (in the DSL) a greater amount of TKE is produced than dissipated, while farther from the wall (in the DCSL), dissipation exceeds production, and that a crossover occurs in the transition zone, at a $-z/L$ of about 0.1. Of course, dissipation must equal production when integrated over the depth of the ABL for a stationary and homogenous flow. This fact seems more in line with the present result of dissipation being less than production near the wall and exceeding production away from the wall, as opposed to the earlier view of dissipation matching production near the wall and exceeding production away from the wall.

Acknowledgements. The authors wish to thank Anthony Cahill and Mike Mata for their assistance in the field, Scott Tyler for his logistical help at Owens Valley, and the four anonymous reviewers for their insightful comments. This research has been supported and financed, in part, by the National Science Foundation (EAR-93-04331), CA State Salinity Drainage Task Force, Kearney Foundation, CA Water Resources Center (W-182), the UC Davis Superfund grant (5P42ES04699-07), the Great Basin Air Pollution Control District, and the NASA Graduate Student Fellowship in Global Change Research program.

References

Albertson, J.D., M.B. Parlange, G.G. Katul, C.-R. Chu, H. Stricker, and S. Tyler, Sensible heat flux from arid regions: A simple flux-variance method, *Water Resour. Res.*, 31, 969-973, 1995.

Albertson, J.D. , G. Kiely, and M.B. Parlange, Surface fluxes of momentum, heat, and water vapor, in *Radiation and Water in the Climate System*, edited by E.Raschke, *NATO ASI Ser. I: Global Environ. Change*, pp. 59-82, Springer-Verlag, New York, 1996.

Anselmet, F., Y. Gagne, E.J. Hopfinger, and R.A. Antonia, High-order velocity structure functions in turbulent shear flows, *J. Fluid Mech., 140*, 63-89, 1984.

Batchelor, G.K., Pressure fluctuations in isotropic turbulence, *Proc. Cambridge Philos. Soc., 47*, 359-374, 1951.

Bernstein, A.B., A new dimensional approach to the flux-gradient approach near the ground, *Q. J. R. Meteorol. Soc., 92*, 560-566, 1966.

Betchov, R., and A.M. Yaglom, Comments on the theory of similarity as applied to turbulence in an unstably stratified fluid, (in Russian), *Izv. Akad. Nauk. SSSR Fiz. Atmos. Okeana, 7*, 1270-1279, 1971. *(Izv. Acad. Sci. USSR Atmos. Oceanic Phys.*, Engl. Transl., *7*, 829-834, 1971).

Brutsaert, W., *Evaporation Into the Atmosphere*, 299 pp., Kluwer Acad., Norwell, Mass., 1982.

Brutsaert, W., Stability correction functions for the mean wind speed and temperature in the unstable surface layer, *Geophys. Res. Lett., 19*, 469-472, 1992.

Businger, J.A., J.C. Wyngaard, Y. Izumi, and E.F. Bradley, Flux profile relationships in the atmospheric surface layer, *J. Atmos. Sci., 28*, 181-189, 1971.

Champagne, F.H., C.A. Friehe, J.C. LaRue, and J.C. Wyngaard, Flux measurements, flux estimation techniques, and fine-scale turbulence measurements in the unstable surface layer over land, *J. Atmos. Sci., 34*, 515-530, 1977.

Deacon, E.L., The measurement of turbulent transfer in the lower atmosphere, *Adv. Geophys., 6*, 211-228, 1959.

Deacon, E.L., The streamwise Kolmogorov constant, *Boundary Layer Meteorol., 42*, 9-17, 1988.

deLeonibus, P.S., and L.S. Simpson, Dissipation observations of drag coefficients over the open ocean, *IEEE J. Oceanic Eng., OE-12*, 296-300, 1987.

Dyer, A.J., A review of flux-profile relations, *Boundary Layer Meteorol., 1*, 363-372, 1974.

Edson, J.B., C.W. Fairall, P.G. Mestayer, and S.F. Larssen, A study of the inertial-dissipation method for computing air-sea fluxes, *J. Geophys. Res., 96*, 10, 689-10, 711, 1991.

Eichinger, W.E., D.I. Cooper, D.B. Holtkamp, R.R. Karl Jr., C.R. Quick, and J.J. Till, Derivation of water vapour fluxes from lidar measurements, *Boundary Layer Meteorol., 63*, 39-64, 1993.

Fairall, C.W., and S.E. Larsen, Inertial-dissipation methods and turbulent fluxes at the air-ocean interface, *Boundary Layer Meteorol., 34*, 287-301, 1986.

Frenzen, P., and C.A. Vogel, The turbulent kinetic energy budget in the atmospheric surface layer: A review and an experimental reexamination in the field, *Boundary Layer Meteorol., 60*, 49-76, 1992.

Frisch, U., *Turbulence: The Legacy of A.N. Kolmogorov*, 296 pp., Cambridge Univ. Press, New York, 1995.

Hogstrom, U., Analysis of turbulence structure in the surface layer with a modified similarity formulation for near neutral conditions, *J. Atmos. Sci., 47*, 1949-1972, 1990.

Kader, B.A., Three-level structure of an unstably stratified atmospheric surface layer, *Izv. Acad. Sci. USSR Atmos. Oceanic Phys.*, Engl. Transl., *24*, 907-919, 1988.

Kader, B.A., Determination of turbulent momentum and heat fluxes by spectral methods, *Boundary Layer Meteorol., 61*, 323-347, 1992.

Kader, B.A., and V.G. Perepelkin, Effect of unstable stratification on the wind speed and temperature profiles in the surface layer, *Izv.Acad. Sci. USSR Atmos. Oceanic Phys.*, Engl. Transl., *25*, 583-588, 1989.

Kader, B.A., and A.M. Yaglom, Mean fields and fluctuation moments in unstably stratified turbulent boundary layers, *J. Fluid Mech.*, 212, 637-662, 1990.

Kaimal, J.C., Flux and profile measurements from towers in the boundary layer, in *Probing the Atmospheric Boundary Layer*, edited by D.H. Lenschow, pp. 19-28, Am. Meteorol. Soc., Boston, Mass., 1986.

Kaimal, J.C., and J.J. Finnigan, *Atmospheric Boundary Layer Flows*, 289 pp. Oxford Univ. Press, New York, 1994.

Kaimal, J.C., J.C. Wyngaard, and D.A. Haugen, Deriving power spectra from a three-component sonic anemometer, *J. Appl. Meteorol., 7*, 827-837, 1968.

Katul, G.G., C.-R. Chu, M.B. Parlange, J.D. Albertson, and T.A. Ortenburger, The large scale spectral characteristics of stratified atmospheric surface layer flows, *J. Geophys. Res., 100*, 14,243-14,255, 1995.

Kiely, G., J.D. Albertson, M.B. Parlange, and W.E. Eichinger, Convective scaling of the average dissipation rate of temperature variance in the atmospheric surface layer, *Boundary Layer Meteorol., 77*, 267-284, 1996.

Kolmogorov, A.N., The local structure of turbulence in incompressible viscous fluid for very large Reynolds number, *Dokl. Akad. Nauk SSSR, 30*, 301-303, 1941.

Kraichnan, R.H., Turbulent cascade and intermittency growth, *Proc. R. Soc. London, Sec. A, 434*, 65-78, 1991.

Leavitt, E., and C.A. Paulson, Statistics of surface layer turbulence over the tropical ocean, *J. Phys. Oceanogr., 5*, 143-156, 1975.

McBean, G.A., and J.A. Elliott, The vertical transport of kinetic energy by turbulence and pressure in the boundary layer, *J. Atmos. Sci., 32*, 753-766, 1975.

McBean, G.A., R.W. Stewart, and M. Miyake, The turbulent energy budget near the surface, *J. Geophys. Res., 76*, 6540-6549, 1971.

Meneveau, C., and K.R. Sreenivasan, The multifractal nature of turbulent energy dissipation, *J. Fluid Mech., 224*, 429-484, 1991.

Monin, A.S., and A.M. Yaglom, *Statistical Fluid Mechanics*, vol. I, edited by J. Lumley, 768 pp., MIT Press, Cambridge, Mass.,1971.

Monin, A.S., and A.M. Yaglom, *Statistical Fluid Mechanics*, vol. II, edited by J. Lumley, 874 pp., MIT Press, Cambridge, Mass.,1975.

Panton, R.L., *Incompressible Flow*, 780 pp., Wiley-Interscience, New York, 1984.

Parlange, M.B., and W. Brutsaert, Regional shear stress of broken forest from radiosonde wind profiles in the unstable surface layer, *Boundary Layer Meteorol., 64*, 355-368, 1993.

Parlange, M.B., and G.G. Katul, Watershed scale shear stress from tethersonde wind profile measurements under near neutral and unstable atmospheric stability, *Water Resour. Res., 31*, 961-968, 1995.

Skupniewicz, C.E., and K.L. Davidson, Hot-film measurements from a small buoy: Surface wind estimates using the inertial dissipation method, *J. Atmos. Oceanic Technol., 8*, 309-322, 1991.

Stull, R., *An Introduction to Boundary Layer Meteorology*, 666 pp., Kluwer Acad., Norwell, Mass., 1988.

Taylor, G.I., The spectrum of turbulence, *Proc. R. Soc. London, Sec. A*, *CLXIV*, 476-490, 1938.

Tennekes, H., and J. Lumley, *A First Course in Turbulence*, 300 pp., MIT Press, Cambridge, Mass., 1972.

von Karman, T., and L. Howarth, On the statistical theory of isotropic turbulence, *Proc. R. Soc. London, Sec. A*, *164*(917), 192-215, 1938.

Wyngaard, J.C., Lectures on the planetary boundary layer, in *Mesoscale Meteorology: Theory, Observations and Models*, edited by D.K. Lilly and T. Gal-Chen, pp. 603-650, D. Reidel, Norwell, Mass., 1983.

Wyngaard, J.C., Measurement physics, in *Probing the Atmospheric Boundary Layer*, edited by D.H. Lenschow, pp. 5-18, Am. Meterol. Soc., Boston, Mass, 1986.

Wyngaard, J.C., and O.R. Cotè, The budgets of turbulent kinetic energy and temperature variance in the atmospheric surface layer, *J. Atmos. Sci.*, *28*, 190-201, 1971.

Zilitinkevich, S.S., Turbulence and diffusion in free convection (in Russsian), *Izv., Akad. Nauk. SSSR Fiz. Atmos. Okeana*, *7*, 1263-1269, 1971. (*Izv. Acad. Sci. USSR Atmos. Oceanic Phys.*, Engl. Transl., *7*, 825-828, 1971).

Zilitinkevich, S., A generalized scaling for convective shear flows, *Boundary Layer Meteorol.*, *70*, 51-78, 1994.

J. D. Albertson, Department of Environmental Sciences, University of Virginia, Charlottesville, VA 22903. (e-mail: jdalbertson@virginia.edu).

W. E. Eichinger, Institute of Hydraulic Research, University of Iowa, 404 Hydraulics Laboratory, Iowa City, IA 52242.

G. Kiely, Department of Civil Engineering, University College, Cork, Ireland.

M. B. Parlange, Department of Geography and Environmental Engineering, The Johns Hopkins University, Baltimore, MD 21218.

(Received November 30, 1994; revised July 15, 1996; accepted August 6, 1996.)